Arc Sensing for Defects in Constant-Voltage Gas Metal Arc Welding

A method for detecting flaws in automatic, constant-voltage gas metal arc welding using the process current and voltage signals was developed

BY T. P. QUINN, C. SMITH, C. N. McCOWAN, E. BLACHOWIAK AND R. B. MADIGAN

ABSTRACT. A method for detecting flaws in automatic, constant-voltage gas metal arc welding using the process current and voltage signals was developed. Seven algorithms process the current and voltage signals to give quality parameters. A defect-detection algorithm processes the quality parameters and flags welds that are different from a baseline. The baseline is constructed from the recorded quality parameters of previously made, defect-free welds. Two series of tests were conducted to test the sensitivity of the algorithms for defects and to test the entire sensor system in production. In the first series, on a 3-mm lap joint, the algorithms detected a lack of shielding gas, oily parts and melt-through from inadequate part cross section, but could not detect off-joint welding. The algorithms showed a mixed sensitivity to melt-through from large root openings. In production tests, 520 welds were monitored. The defect detection algorithm was tuned on data from the first 82 welds. The sensor flagged five of the six defects monitored and did not flag any defect-free welds. The defect not detected was a small pore, < 3 mm diameter.

Introduction

This article describes a method for detecting flaws in automatic, constant-voltage, gas metal arc welding (GMAW) using the process current and voltage signals. In many situations where automation is used to make a large volume of parts, the operator cannot closely monitor the weld as it is being made; the operator is either in charge of several stations or must stay clear of the robotic arm. Therefore, even gross defects cannot be detected until after the part is completely welded, and each part must undergo postweld inspection. Even if the postweld inspection is a simple visual check, the cost of another processing step is incurred. Therefore, there is need for a system to assess the quality of the weld as it is being made.

T. P. QUINN and C. N. McCOWAN are with the National Institute of Standards and Technology, Boulder, Colo.; C. SMITH is with Tower Automotive, Milwaukee, Wis.; E. BLACHOWIAK is with A. O. Smith Corp., Milwaukee, Wis.; and R. B. MADIGAN is with Arc Logic, Breckenridge, Colo.

Many sensing systems have been designed to reduce defects in automatic GMAW (Refs. 1–4). To reduce problems caused by welding out-of-joint, sensors that track the joint using the current or voltage signal, video imaging and laser-based structured-light machine vision have been developed (Ref. 5). Other sensors are used for process control (Refs. 6–8). A drawback to some of these sensing systems is that additional hardware must be added to the end of the torch. This is not possible in some automatic applications in which the fixtures holding the parts in place allow for only minimal torch clearance. The system described here uses the process current and voltage signals and therefore requires no additional hardware be added to the torch.

Through-the-arc sensing (a sensor that uses the process current and voltage signals alone) has developed from data-logging devices that record the current, voltage and even wire feed speed. Kohn and Siewert (Ref. 9) studied the characteristics of short-circuit transfer and related the stability of the electric pattern to the quality of the weld. Johnson, *et al.* (Ref. 7), investigated other transfer modes using the current and voltage. We have developed arc stability algorithms for pulsed-current GMAW (Ref. 10). Ludewig, *et al.* (Ref. 11), integrated the Fourier transform of the current and voltage from 0 to 200 Hz as a measure of the quality of the weld. They also measured the raw derivatives and the raw standard deviation of the current and voltage. They set absolute thresholds on these quality parameters to determine whether a weld is defective. Sanders, *et al.* (Ref. 12), used a nonsequential moving average of the current, voltage, short-circuit ("dipping") frequency with absolute limits to detect defects. Rehfeldt and Polte (Ref. 13) used probability density distributions of the current and voltage and detected defects with a fuzzy logic method.

KEY WORDS

Algorithm
Constant Voltage
Defects
GMAW
Monitoring
Process Control
Sensors

In the research presented here, we have tried to design signal processing methods sensitive to irregularities in the weld and to develop a technique to flag defective welds. Specifically, the objectives of this paper are 1) to describe a series of algorithms that operate on the current and voltage signals in constant-voltage, GMAW that can assess the state of the process; 2) describe a method that can be used to determine the quality of a weld from any sensing system for use in automatic welding of mass-produced parts; and 3) report on the production trials of the sensing system developed in 1) and 2).

Methods

The methods for sensing constant-voltage GMAW are those described in Ref. 14 and are similar to those in Ref. 10 for sensing pulsed-current GMAW. The methods for constant-voltage GMAW will be described briefly here for clarity; details of the algorithms can be found in the appendix. The hardware for the system consists of a voltage probe, current transducer, isolation backplane and computer — Fig. 1. The current and voltage signals are continuously sampled by the computer (at a sampling frequency usually greater than 4000 samples/s). Seven algorithms process blocks of the data to produce the quality parameters. The number of samples N in each block of data determines the update rate of the quality parameters (typically $\frac{1}{32}$ s). The

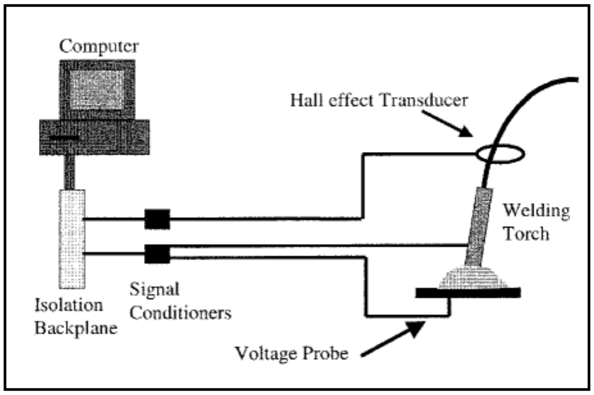

Fig. 1 — Hardware configuration of the sensor.

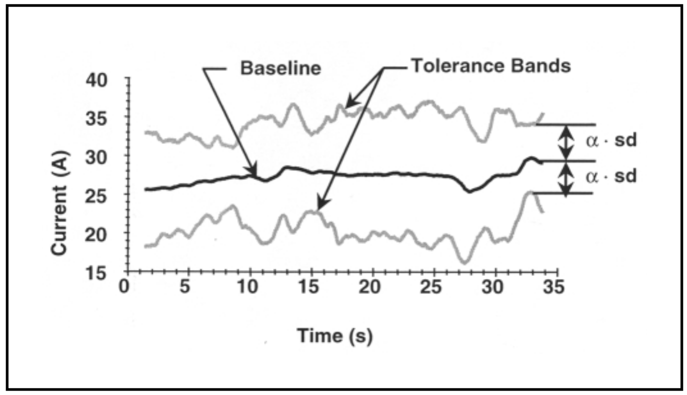

Fig. 2 — Tolerance bands are determined as a fraction α of the standard deviation of the quality parameter or as some fraction of the baseline β (not shown). The concept is illustrated here with the running average of the current.

quality parameters are then acted on by a routine that determines whether the weld has a defect.

The seven algorithms for constant-voltage GMAW are (1) the running average and standard deviation of current, (2) the running average and standard deviation of voltage, (3) the running average and standard deviation of resistance,(4) the arc condition number, (5) the voltage trend, (6) the current trend and (7) the short-circuit frequency and standard deviation of the short-circuit frequency. The resistance of the process is found by dividing the voltage sample by the corresponding current sample. The averages and standard deviations of the current, voltage and resistance are calculated over the *N* samples in each block. The arc condition number is a measure of the low frequency (less than 200 Hz) stability of the process. The short-circuit frequency and standard deviation are calculated by identifying the short circuit events in each block. The trend in the current and voltage are found by fitting a line to the running average of the current and voltage.

Defect Detection

The defect detection method compares the weld in question to a baseline record. A baseline record is constructed from the recordings of the quality parameters made during a number of defect-free welds by averaging the defect-free welds' quality parameters and smoothing the result. A threshold based on a fraction of the standard deviation of the quality parameters (α) or on a fraction of the value of the quality parameter (β) is set — Fig. 2. Since excursions of the quality parameters beyond the threshold for short periods of time may be acceptable, a weld is declared defective if the quality parameter is out of the threshold for some fraction of an interval that moves with the data (if M_f out of N_f points are out of tolerance). Therefore, three numbers are needed for defect-detection for each quality parameter: N_f, M_f and α or β. A detailed description of the detection method is given in the appendix.

Experiments

Series I

Two series of experiments were conducted. The first series of tests was designed to test the sensitivity of the quality parameters to various defects. Defects were intentionally made on production parts in test runs in an automotive parts factory. Five defect conditions were tested: 1) lack of shielding gas, 2) oily parts, 3) the torch located off of the joint, 4) thin part sections causing melt-through and 5) large root openings (Table 1). Two test welds were made under normal conditions. For all test conditions, an articulated arm robot fitted with a GMAW torch with a constant-voltage power supply welded a fillet weld in a lap joint of 3-mm-thick mild steel — Fig. 3. Mild steel wire (1.2 mm diameter) was used with an 85% Ar -15% CO_2 shielding gas. The travel speed was approximately 35 mm/s; the wire feed speed was approximately 201 mm/s; the voltage was set at approximately 22 V for a "buried-arc" transfer mode (a 2–3 mm arc length with bridging transfer). The weld duration was about 32 s on parts of complex geometry.

The current and voltage signals for these tests were sampled at 6000 samples per second and recorded for later processing. The current was measured with a Hall-effect transducer with an absolute (total) error of 1%. The voltage between the torch and the grounding fixture was measured within 0.5% absolute error.

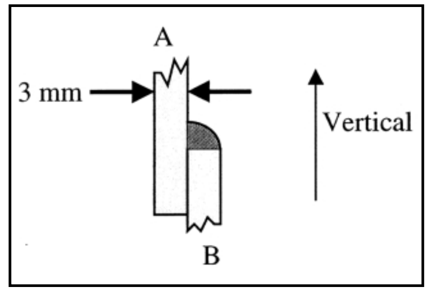

Fig. 3 — Joint geometry and welding position of parts used in Series I and Series II tests.

Series II

The second series of experiments was designed to test the defect-detection algorithm. Experiments were conducted in two parts on the production floor. In the first part the raw current and voltage signals were again recorded at 6000 samples per second. The same joint geometry and welding conditions as in Series I were used. We monitored 63 welds for each of two kinds of parts that had slightly different geometry: Part A and Part B. The welds monitored were made on three different shifts of the production floor operation. Part A and B were made on the first shift; only Part A was made on the second shift, and only Part B was made on the third shift. The weld path for both parts involved compound curves. The parts were visually inspected for defects such as surface porosity and melt-through in a manner similar to production quality checks.

The raw data were passed through the sensor algorithms off-line. The constants needed for the defect detection algorithm N_f, M_f and α or β for each of the seven quality parameters were found by processing the first 82 welds; the parameters were set so that defective welds were

Table 1 — Procedures and Number of Parts for Welds Made for Series I

Case	Welding Condition	Procedure	Number of Parts
1	Lack of shielding gas	The valve that controlled shielding gas flow started to close after 10 s of welding. The valve was completely closed after 20 s of welding and remained closed for the duration of the weld.	3
2	Oily parts	The section of the parts that corresponded to the first 9 s of weld and last 6 s of the weld remained clean. The section of the parts from 9 to 24 s was "painted" with light hydraulic oil of approximately increasing amounts: the first part had a light amount increasing to the last of the four parts, which was dripping with oil.	4
3	Mislocated torch	The robot was programmed to weld in the joint for the first 6 s, out of the joint on the single cross section (Side A, Fig. 3) from 6 to 12 s, in the joint from 12 to 18 s, out of the joint on the double cross section (Side B, Fig. 3) from 18 to 24 s, and in the joint from 24 to 32 s. When the torch was to weld out of the joint, the distance out was the same on Side A or Side B. For the first three parts, it was 1.5 mm out of the joint; for the final three parts it was 2 mm out of the joint.	6
4	Melt-through	The single cross section (Side A, Fig. 3) was thinned to approximately 2 mm for the first two welds. To ensure a melt-through would be observed, the cross section for the final weld was thinned to approximately 1.5 mm.	3
5	Large root opening	Side A in Fig. 3 was deformed with a ball peen hammer at several locations, to cause an uneven root opening after the hydraulic clamps that held the part were closed.	1
6	Normal	Welds were made under normal welding conditions.	2

flagged and defect-free welds were not flagged. The optimal constants were found by "cut and try" trials using batch processing. The defect-detection algorithm was then tested for robustness by applying it to the final 44 welds using the constants found for the first 82 welds. A baseline series was constructed from 10 defect-free welds ($N_b = 10$, see appendix) at the start of each shift. A smoothing window of 0.625 s ($N_s = 10$, see appendix) was chosen based on the travel speed and changes in geometry of the part. The first and last 1.3 s of the weld were ignored due to the variability in the starts and stops.

In the second part of Series II, a software package implementing the defect-detection algorithm was coupled with the sensing hardware and brought to a second production floor. In this case, defects were flagged on-line. The constants (N_f, M_f, and α and β) found in the first series of tests were used in the defect detection algorithm for a weld that lasted approximately 2 s. The joint, power source and welding conditions were approximately the same as for Part A and B above. Four-hundred welds were monitored on three production shifts. A baseline series was constructed (as above) with the first ten welds, which were defect-free and used for all of the shifts. The first 0.5 s of weld were ignored; no data were ignored at the end of the weld.

Results and Discussion

Series I

The quality parameters were sensitive to loss of shielding gas, dirty parts and melt-throughs due to thin part cross sections. In tests when the gas was turned off (Case 1), the current, voltage and resistance averages did not vary greatly from the values found during the control welds (Case 6) — Fig. 4. In Fig. 4, the current was less than 2.1 standard deviations away from the mean of the control welds and the voltage was less than 0.5 standard deviation away. (To make realistic comparisons, the quality parameters are shown with the thresholds determined from the Series II welds, Table 2). However, the arc condition number increased by as much as 857% above the baseline (140% out of tolerance) when the gas was turned off. When the gas was off, the joint showed gross surface porosity and incomplete fusion.

The arc condition number also was sensitive to the disturbance in the arc cre-

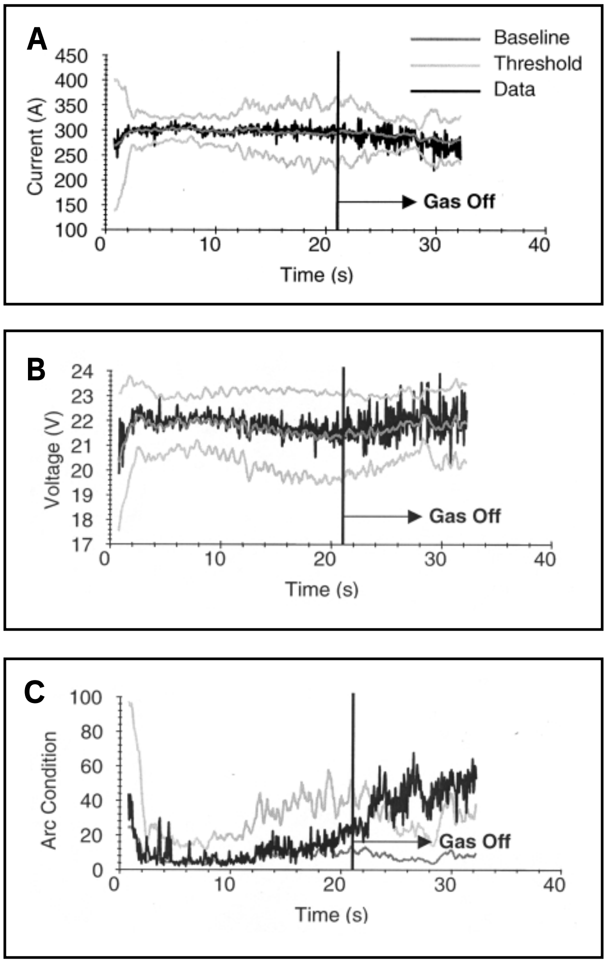

Fig. 4— The (A) current, (B) voltage and (C) arc condition number during a Series I, Case 1 weld. The gas was turned off at approximately 21 s. The threshold values were determined from the Series II tests. The baseline was constructed from the Case 6 welds with N_s = 5 (see appendix). The current and voltage largely remain in bounds while the arc condition number is as much as 857% above the control.

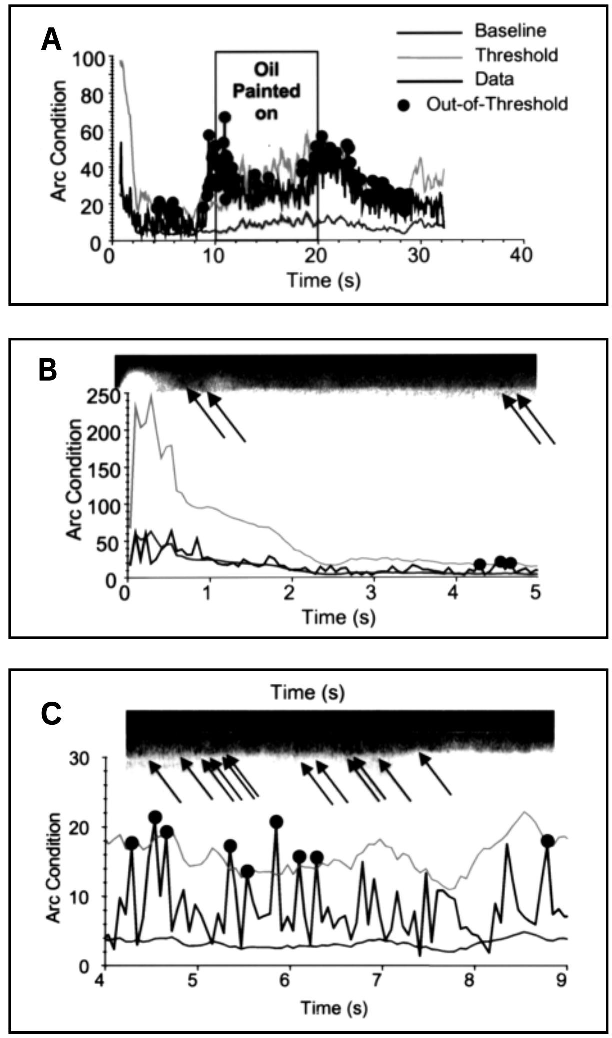

Fig. 5 — The arc condition number for a weld with (A) a light amount of oil painted on the surface. The weld was X-rayed and subsurface porosity is identified with arrows (B and C). The rise in the arc condition number prior to the weld reaching the oil corresponds to subsurface porosity.

ated by the oil that was painted on the parts in Case 2 — Fig. 5A. There was a rise in the arc condition number before the arc reached the area where the oil was painted. No defects could be identified with visual inspection for this area of the weld, but X-ray evaluations of the welds in Case 2 show the rise in the arc condition number can be associated with subsurface porosity in the part (Fig. 5B and C). The porosity was probably due to oil vapors inducted into the arc or oil wicking along the joint. Surface porosity was evident in the area where the oil was painted (Fig. 5, from 10–20 s); the arc condition number remained high in this area.

The quality parameters were less sensitive to welding off the joint centerline. The current was higher (resistance lower) when on the double thickness of material (Fig. 3, side B) but remained within about one standard deviation of the baseline value — Fig. 6. Through-the-arc sensing of the joint position (Ref. 5) has been shown to be successful only with deeper joint configurations because the effective CTWD is changing by a relatively small amount as the torch is moved out of this joint. The practical restrictions that apply to through-the-arc joint tracking will apply here. When the torch was welding on the single-thickness side (Fig. 3, side A), the current was about the same as the baseline value.

Table 2 — The Best Defect Detection Constants Found Using the First 82 Welds of Series II, Part 1

Quality Parameter	M_f	N_f	α	β
Average Current	3	5	2	—
Average Voltage	3	3	0.4	—
Average Resistance	2	2	1.75	—
Arc Condition Number	2	2	—	2.9
Short-Circuit Frequency	10	10	1.5	—
Voltage Trend	6	10	—	20
Current Trend	6	10	—	140

Melt-through defects caused by thinning the cross section of the part (Case 4)

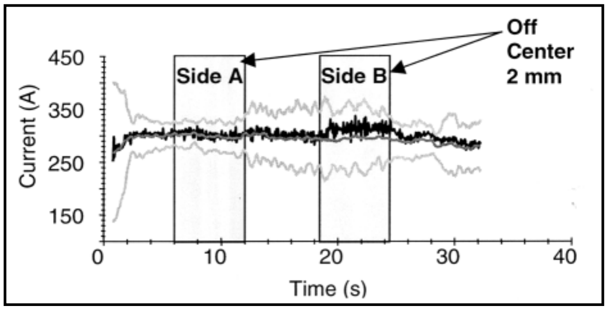

Fig. 6 — The current average while welding in the joint centerline, then 2 mm away from the centerline on side A (Fig. 3), then in the centerline, then off the centerline 2 mm on side B, then again in the centerline. The same legend is used as in Fig. 5.

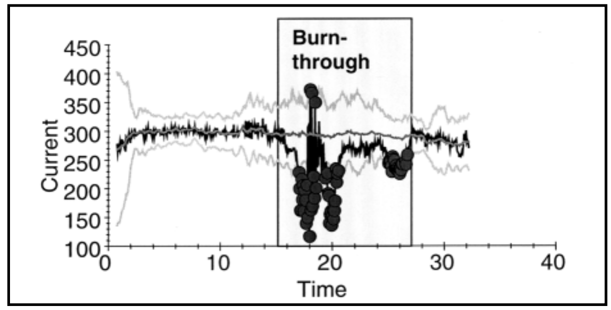

Fig. 7 — The current during a melt-through caused by thinning the wall of the part. The same legend is used as in Fig. 5.

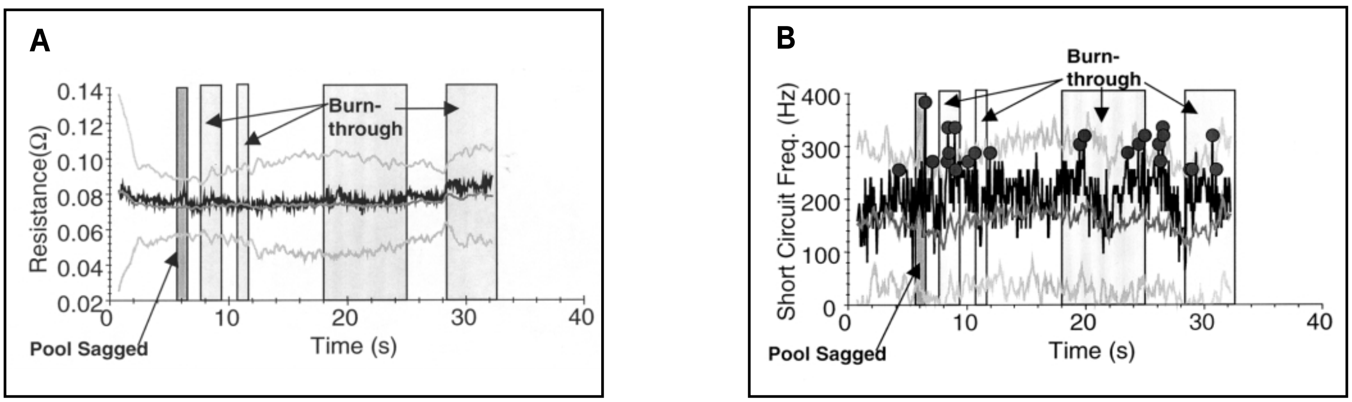

Fig. 8 — The resistance (A) and short circuit frequency (B) during the weld with large root openings (Case 5). The short circuit frequency is sensitive to the first, second, fourth and fifth defects but missed the third defect and showed sensitivity where no defect was detected visually. No other quality parameter (see resistance, part A) is sensitive to the defects. The same legend is used as in Fig. 5.

were sensed by the quality parameters — Fig. 7. However, the quality parameters were sensitive to some, but not all, of the defects that occurred for the Case 5 weld with the large root openings — Fig. 8. If the weld pool falls through after the arc has passed, the sensor will not be able to detect the defect.

For the defect conditions tested, the trend in the current and voltage gave no indication of any of the defects. The arc condition number was the most sensitive to defects.

Series II

Part 1

Of the 126 welds monitored in Part 1, five defects were identified by visual inspection. One defect (surface porosity) was about 70 mm in length; the other four were small skips or pores about 3 mm diameter. The other 121 welds were defect-free on visual inspection. The first 82 welds (from which the defect detection constants were found) had four defective welds. The defect-detection constants (Table 2) flagged three of the four defective welds of the first 82 and did not flag any of the defect-free welds (Table 3). There was a single small defect in the final 44 welds. The algorithm flagged this weld (Fig. 9) and did not flag any of the 43 others.

For the reference series shown in Fig. 9, the arc condition number is about four times greater in the last 20 s of weld than it is from 4 to 10 s. If an absolute limit on the arc condition number were used for defect detection, it would have to be set around 60 to accommodate this intentional change in the welding parameters. The defective weld shown in Fig. 9 would not have been flagged with this absolute limit.

One of the difficulties with the defect-detection algorithm is that, with several quality parameters, there are many constants to find. To speed the selection of the defect-detection constants, the 2 s of the current and voltage data during which the defect occurred for each of the four defective welds were concatenated together with 2 s worth of data from defect-free welds that showed large excursions from the baseline series; this formed a single composite series. The corresponding sections of the baseline series were put together to form a composite baseline series. The software we wrote allowed us to plot the seven quality parameters of the composite series against the seven quality parameters of the baseline composite together with the thresholds. Using the composite series, the constants were found within a few (< 10) iterations.

When we selected the defect detection constants, we used the quality acceptance criteria used on the factory floor. If a different quality standard was used, the defect detection constants could be modified to make the defect-detection system more sensitive. To determine the defect-detection constants, production floor data are required, both the quality parameter data and a record of when the defects occurred.

Part 2

Since the first 358 welds monitored in Part 2 were free of defects, the torch position was changed on number 359 to cause a melt-through and then returned to its original position for the rest of the welds. No defects were observed on the subsequent 41 welds. The defect-detection algorithm flagged the single defec-

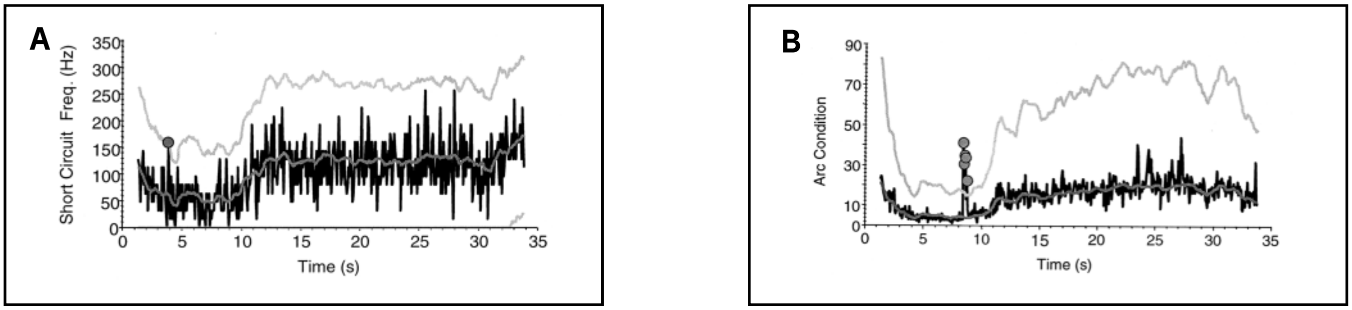

Fig. 9 — The arc condition and short circuit frequency quality parameters for a weld with a defect at 8.7 s. Because of the settings of the constants in Table 1, the defect detection algorithm flagged the weld because of the arc condition number (more than 2 out of 2 out) but not because of the short circuit frequency (only 1 out of 10 out). The same legend is used as in Fig. 5.

tive weld (arc condition, resistance and voltage flagged the weld). The algorithms did not flag any of the defect-free welds using the same defect detection constants identified in Part 1 (Table 2).

The overall statistics for Series II tests were five of six welds with defects were flagged, and 520 of 520 defect-free welds were not flagged. The defect that was not flagged was caused by a piece of spatter buildup on the gas nozzle falling into the weld pool causing a small pore and a lump in the weld bead.

Table 3 — The Quality Parameters That Flagged the Five Defects in Series II, Part 1, Using the Defect Detection Constants in Table 2

Defect Description	1 3-mm pore	2 3-mm pore	3 3-mm pore	4 70-mm surface porosity	5 3-mm pore
Average Current				•	
Average Voltage			•	•	
Average Resistance	•		•	•	
Arc Condition Number				•	•
Short-Circuit Frequency					
VoltageTrend				•	
Current Trend				•	

Conclusions

1) A sensing strategy for welding defects has been developed. Algorithms process the recorded current and voltage signals to produce quality parameters. The quality parameters are then compared to a variable threshold based on records of defect-free welds.

2) The weld sensing system was sensitive to melt-throughs due to thin sections, loss of shielding gas and oily parts that cause surface and subsurface porosity. The system could not consistently detect off-joint welds for the 3-mm leg-length fillets tested or large root openings causing melt-throughs.

3) With the defect-detection algorithm in place, the entire system was tested in production on two factory floors. Five of six defective welds were flagged; 520 defect-free welds were not flagged.

4) The raw current and voltage signals are not enough to detect all defects in constant-voltage GMAW under the conditions studied. When the signals are passed through the described algorithms, the sensitivity to defects is increased.

References

1. Araya, T., and Saukawa, S. 1992. Recent activities on sensing and adaptive control of arc welding. *Proc. 3rd International Conference on Trends in Welding Research*, eds. S. A. David and J. M. Vitek, ASM International, Materials Park, Ohio, pp. 833–842.

2. Smartt, H. B. 1992. Intelligent sensing and control of arc welding. *Proc. 3rd International Conference on Trends in Welding Research*, eds. S. A. David and J. M. Vitek, ASM International, Materials Park, Ohio, pp. 843–851.

3. Sicard, P., and Levine, M. D. 1988. An approach to an expert robot welding system. *IEEE Transactions on Systems, Man and Cybernetics* 18(2):204–222.

4. Hanright, J. 1986. Robotic arc welding under active control — a survey of current technology. *Welding Journal* 65(11):19–24.

5. Richardson, R. W. 1986. Robotic weld joint tracking systems — theory and implementation methods. *Welding Journal* 65(11):43–51.

6. Madigan, R. B., and Quinn, T. P. 1993. Control of arc length during gas metal arc welding using arc light sensing. *Proc. Modeling and Control of Joining Processes*, ed. T. Zacharia, American Welding Society, Miami, Fla., pp. 125–133.

7. Johnson, J. A., Carlson, N. M., Smartt, H. B., and Clark, D. E. 1991. Process control of GMAW: sensing of metal transfer mode. *Welding Journal* 70(4):91-s to 99-s.

8. Song, J.-B., and Hardt, D. E. 1993. Closed-loop control of weld depth using a thermally based depth estimator. *Welding Journal* 72(10):471-s to 478-s.

9. Kohn, G., and Siewert, T. A. 1986. The effects of power supply response characteristics on droplet transfer of GMAW welds. *Proc. International Conference on Trends in Welding Research*, ed. S. A. David, ASM International, Materials Park, Ohio, pp. 299–302.

10. Siewert, T. A., Madigan, R. B., and Quinn, T. P. 1993. Sensing of Gas Metal Arc Welding Process Characteristics for Welding Process Control. United States Patent No. 5,221,825.

11. Ludewig, H. W., Siwicke, J. H., Kilty, A. L., Wallace, B. L., Haytcher, S. A., and Rees, D. E. 1996. Method for Arc Welding Fault Detection. United States Patent No. 5,521,354.

12. Sanders, L., West, M., and Norrish, J. 1998. Real-time irregularity detection in gas metal arc welding. *Proc. 8th International Conference on Computer Technology in Welding,* American Welding Society, Miami, Fla.

13. Rehfeldt, D., and Polte, T. 1998. Systems for processing monitoring and quality assurance in welding. *Proc. 8th International Conference on Computer Technology in Welding*, American Welding Society, Miami, Fla.

14. Quinn, T. P., and Madigan, R. B. 1998. Sensing of Arc Welding Process Characteristics for Welding Process Control. United States Patent No. 5,756,967.

Appendix

Quality Parameters

The seven quality parameters are calculated by sampling the current and voltage continuously at a sampling rate *f* (typically > 4000 samples per second). After every *N* samples, the sampled current and voltage data are passed through several algorithms which produce quality

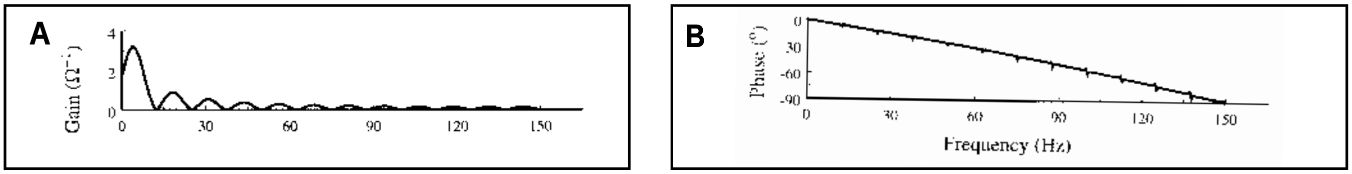

Fig. 10 — The transfer function for the arc condition number. Derived from simulation of a 150 A, 22 V arc with added noise. f = 6000, N = 375, M = 12.

parameters every $T = N/f$ periods (T is typically 1/32 s). The running average of the current I_{av} and standard deviation of the current I_{st} and the running average and standard deviation of the voltage (V_{av} and V_{st}) are calculated with the N samples in the period. Each term in the resistance series is calculated as $R_i = V_i / I_i$, where i refers to the ith sample. (If $I_i = 0$, then $R_i = V_i/10^{-6}$.) The running average and standard deviation of the resistance (R_{av} and R_{st}) are calculated over the R_i.

The arc condition number is a measure of the low-frequency stability of the arc. It is calculated by dividing the N samples of the resistance series into M subintervals of length m and calculating the average resistance in each subinterval:

$$R_j^s = \frac{1}{m}\sum_{i=j}^{j+m} R_i, \qquad (1)$$

where R_j^s is the series of average resistances in the subintervals. The arc condition number is calculated as

$$G = \frac{\sqrt{\frac{1}{M-1}\sum_j \left(R_j^s - R_{av}\right)^2}}{R_{av}}, \qquad (2)$$

the standard deviation of the R_j^s divided by the overall average R_{av}. The arc condition number operation is equivalent to a low-pass filter (Fig. 10) and is computationally efficient.

The current and voltage trend are found by least-squares fitting a line in time to N_T of the I_{av} and V_{av} (typically N_T = 5). The trends are just the absolute value of the slope of these lines. The update rate for the voltage trend and current trend is then N_T times slower than the other quality parameters.

A threshold is used to determine when short circuit events occur. Because the sampling frequency is relatively high, several voltage points will lie below any reasonable threshold. Therefore, the local minima in the voltage are first found. The minima are identified by fitting n_p voltage samples in the interval t_p with a parabola. (Typically n_p = 4.) If the minimum of the parabola lies within t_p and the minimum is at least some fraction r smaller than either of the end points of the parabola in t_p, the smallest of the n_p points is considered a local minimum. The next n_p points are then examined. The local minima are examined to see if they are below a threshold set as a fraction of the mean voltage in the interval (typically ½ V_{av}). If the minimum is below the threshold, the point is considered to be a short circuit. To calculate the short circuit frequency, the total number of identified shorts is divided by the length of T. The standard deviation of the short circuit frequency is calculated by dividing T into six sub-intervals, calculating a short-circuit frequency for each subinterval and then calculating the standard deviation of these numbers.

Defect Detection

To construct a baseline record, the quality parameter Q is recorded at frequency $1/T$ for at least N_b defect-free welds resulting in ${}^jQ_i$ where i refers to the ith sample in time and j refers to the jth weld. The standard deviation S of the quality parameter is also recorded for the N_b defect-free welds if it is available. To construct the baseline weld, the average over the N_b welds $\hat{Q}$ of the quality parameter at each time increment is first found:

$$\hat{Q}_i = \frac{1}{N_b}\sum_j^{N_b} {}^jQ_i. \qquad (3)$$

The baseline weld series Q_i^b is finally found by smoothing $\hat{Q}$ using a moving average:

$$Q_i^b = \sum_{j=i-N_s/2}^{i+N_s/2} \hat{Q}_j. \qquad (4)$$

N_s is the duration of the moving window and is set to a value large enough that the series is smoothed but not so large that intended changes in Q are smeared out. For example, if the quality parameter is the welding current and the current is reduced as the torch welds around a corner, N_s cannot be made so large that this intentional dip in the current is smoothed. For the start of the weld, $i<N_s/2$, $Q_i^b = \hat{Q}_i$; a similar procedure can be used for the end of the weld.

If S is available, the threshold is first found by computing the average $\hat{S}$ over the N_b welds and then smoothing the result:

$$\hat{S}_i = \frac{1}{N_b}\sum_j^{N_b} {}^jS_i; \qquad (5)$$

$$S_i^b = \sum_{j=i-N_s/2}^{i+N_s/2} \hat{S}_j. \qquad (6)$$

The thresholds are then constructed as

$$T_i^u = Q_i^b + \alpha S_i^b, \quad T_i^l = Q_i^b - \alpha S_i^b, \qquad (7)$$

where T_i^u and T_i^l are the upper and lower threshold, and α is a positive number used to set the threshold width. If S is not available then the thresholds are set as

$$T_i^u = Q_i^b + \beta Q_i^b, \quad T_i^l = Q_i^b - \beta Q_i^b, \qquad (8)$$

where β is used to tune the threshold width. The lower threshold is not needed for the arc condition number.

To allow for short excursions of the quality parameter(s) out of the tolerance band, a weld is not flagged as defective unless M_f out of N_f consecutive Q_i are out of tolerance. For example, if $M_f = 3$ and $N_f = 10$, and Q_{12}, Q_{14}, Q_{19} are out of the tolerance band, then the weld is flagged as defective.